4-2015

A Mechanical Regenerative Brake and Launch Assist Using an Open Differential and Elastic Energy Storage

David H. Myszka
University of Dayton, dmyszka1@udayton.edu

Andrew P. Murray
University of Dayton, amurray1@udayton.edu

Kevin Giaier
University of Dayton

Vijay Krishna Jayaprakash
University of Dayton

Christoph Gillum
Stress Engineering Services

2015-01-1680
Published 04/14/2015

doi:10.4271/2015-01-1680
saealtpow.saejournals.org

A Mechanical Regenerative Brake and Launch Assist using an Open Differential and Elastic Energy Storage

David H. Myszka, Andrew Murray, Kevin Giaier, and Vijay Krishna Jayaprakash
University of Dayton

Christoph Gillum
Stress Engineering Services Inc

ABSTRACT

Regenerative brake and launch assist (RBLA) systems are used to capture kinetic energy while a vehicle decelerates and subsequently use that stored energy to assist propulsion. Commercially available hybrid vehicles use generators, batteries and motors to electrically implement RBLA systems. Substantial increases in vehicle efficiency have been widely cited. This paper presents the development of a mechanical RBLA that stores energy in an elastic medium. An open differential is coupled with a variable transmission to store and release energy to an axle that principally rotates in a single direction. The concept applies regenerative braking technology to conventional automobiles equipped with only an internal combustion engine where the electrical systems of hybrid vehicles are not available. Governing performance equations are formulated and design parameters are selected based on an optimization of the vehicle operation over a simulated urban driving cycle. The functionality of this elastically-based regenerative brake device has been demonstrated on a physical prototype.

CITATION: Myszka, D., Murray, A., Giaier, K., Jayaprakash, V. et al., "A Mechanical Regenerative Brake and Launch Assist using an Open Differential and Elastic Energy Storage," *SAE Int. J. Alt. Power.* 4(1):2015, doi:10.4271/2015-01-1680.

1. INTRODUCTION

A conventional automobile only uses 15-30% of the energy available within the fuel [1]. Increasing fuel prices and control of emissions is prompting automotive manufacturers to increase fuel efficiency. One solution is hybrid vehicles that provide a 60% to 100% gain in fuel economy [2], but only make up approximately 3% of the current market [3]. The vast majority of vehicles on the road are still powered by conventional internal combustion (IC) engines. An increased focus on improving the fuel efficiency in conventional IC vehicles fostered recent developments including the use of alternative fuels [4], reduced friction within engines [5], and continuously variable transmissions [6].

Regenerative braking is the harnessing of kinetic energy typically lost due to braking and converting it to a another form of energy to be used later [7]. Hybrid electric vehicles use a regenerative brake and launch assist (RBLA) system that employs a motor/generator to convert the kinetic energy of the vehicle into electricity when the car is braking. This energy is stored in the batteries and used to propel the vehicle later. Without large battery packs, propulsion motors, hybrid-style RBLA technology is not directly applicable to a conventional vehicle. However, a mechanical RBLA may allow conventional automobiles to benefit from this technology. Further, heavy trailers that do not have a drive train could benefit from RBLA devices.

Various mechanical methods for harnessing and storing the energy have been used as mechanical versions of regenerative braking do not suffer from energy-mode conversion losses. The Kinetic Energy Recovery System utilizes regenerative braking and stores the energy in a carbon-fiber flywheel rotating at speeds up to 65,000 rpm within a vacuum-sealed housing and supported by precision bearings [8]. A Hydraulic Launch Assist uses a pump/motor to convert the kinetic energy to pressurize fluid for refuse trucks and buses with frequent start-stop operation [9]. A mechanical RBLA system using strain energy that is stored and released using a pair of clutches was proposed by Hoppie [10]. Nieman et. al, developed a more compact, spring-based, RBLA mechanism that consisted of gears, clutches, and a ratchet and pawl arrangement [11].

Elastic strain (springs) has been used as a source of energy storage for lifting applications such as garage doors, overhead ladders and automotive hoods. Springs are not commonly considered as a viable option for widespread, high energy storage. At approximately 0.3 kJ/kg (100 ft-lb/lb)[12], the specific energy density of a steel spring is much less than the 100 kJ/kg (35,000 ft-lb/lb) for batteries used in hybrids [13]. Despite having a low energy density, however, springs are able to rapidly release their stored energy. This “power density” can make a spring an attractive alternative for launch assist applications. Additionally, springs are an environmentally friendly alternative to batteries and their well-known design methods provide durable and reliable behavior. Hyperelastic springs, such as rubber,

have much a larger energy density of 12 kJ/kg (4,000 ft-lb/lb)[12], but further research studies must be completed to assess the fatigue life of these materials at high strain. Ongoing research by Hill et al. involves constructing springs from carbon nanotubes, having an energy density of 800 kJ/kg (270,000 ft-lb/lb) greatly exceeding the capacity of batteries [14]. Commercialization of this technology greatly enhances the attractiveness of an elastically-based RBLA system.

This paper explores an alternative to Hoppie's and Nieman's mechanical RBLA systems, which allow conventional vehicles to benefit from regenerative braking. While both concepts have merit, they require precisely sequenced control and have the potential to reflect unwanted shock and vibrations through the vehicle. Additionally, Nieman's concept contains an extension spring that may pose a safety risk. The alternative concept presented in this paper involves an open differential and variable transmission that can smoothly adjust the rate of braking and launching. Additionally, a torsional spring is used to more safely store energy. The remainder of the paper is organized as follows. Section 2 describes the general RBLA concept. The equations governing the design details and vehicle response are developed in Section 3. Section 4 presents a dynamic simulation preformed to confirm the design equations. To have the greatest effect on a vehicle, an optimization to determine ideal design values is presented in Section 5. The development of a benchtop prototype to validate this RBLA concept is described in Section 6.

2. DESCRIPTION OF CONCEPT

The mechanical RBLA concept is intended to be attached to the non-driven axle of a conventional vehicle. It operates in three modes: charge or regenerative braking (RB), discharge or launch assist (LA), and idle. When the RBLA is in charging mode, the spring deforms as it stores energy. In discharge mode, the spring deformation is relieved as stored energy is released. The elastic storage medium can be configured as an extension, torsion or bending element. All of these strain-based storage configurations exhibit a deformation and relaxation cycle that involves a reversal of directions. Since the RBLA is intended to function only when the vehicle is moving, the mechanism must account for these reversals as the axle rotates in a single direction. The idle mode retains any charge in the spring and disengages the RBLA, allowing the vehicle to function as normal.

A sketch of the mechanical RBLA concept is shown in Fig. 1.

The four major components of the RBLA are identified below.

I. A gear drive will transfer motion from the axle to Countershaft A at a fixed ratio. Being external gears, the axle and Countershaft A will rotate in opposite directions.
II. A transmission will transfer motion from the axle to Countershaft B at a variable ratio and has the capacity to vary both above and below the ratio of the gear drive. The transmission is configured such that the axle and Countershaft B will rotate in the same direction.
III. An open differential is configured such that the rotation of the carrier is achieved by combining the motion of Countershaft A and Countershaft B. Since Countershaft A and B rotate in different directions, the differential carrier rotation will depend on the difference between the two countershafts. Differentials are commonly used in automotive applications and proven to be both robust and compact.
IV. The energy storage spring is attached through an energy storage gear pair to the carrier of a differential. As stated, various types of strain-based storage devices could be implemented. In the proposed design of Fig. 1, a torsional spring element is used because less volume is required when the spring is storing energy. Alternatively, an extension band stores energy more efficiently because the material within the spring is at the same stress level. In that case, the spring could be attached to a strap the winds onto a spool attached to the differential carrier.

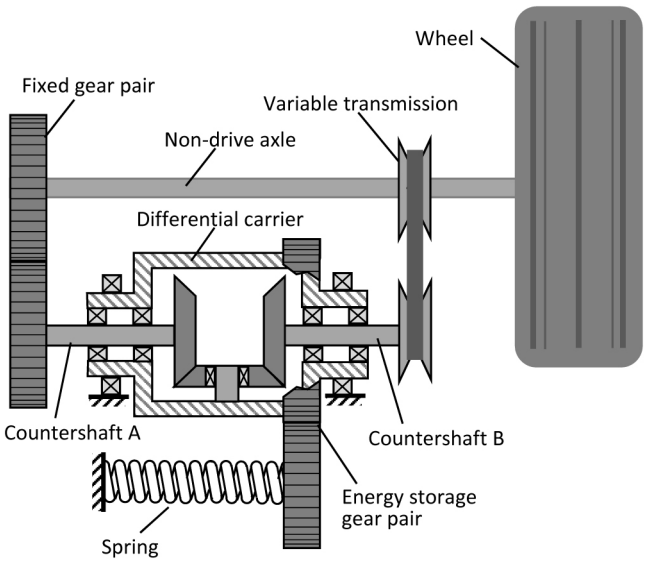

Figure 1. Concept sketch of the RBLA device.

When the variable transmission is adjusted to a ratio equal to the gear drive, Countershaft B rotates at exactly the opposite angular velocity as Countershaft A. The net rotation is zero resulting in no motion of the carrier, and subsequently, the spring. The differential is a critical component of the design, noting that this stasis may be produced even while the axle shaft is rotating. That is, with the RBLA in in this neutral position, the spring neither stores nor releases energy and no additional load is exerted onto the axle.

Moving the ratio of the transmission from the gear ratio causes Countershaft B to rotate with an angular velocity that is not equal and opposite to Countershaft A, which will cause the carrier to rotate. The motion of the carrier can either increase or relieve the deformation of the spring. In the case of an increased deformation, the energy to produce this increase is taken from the axle (slowing the vehicle). As the deformation is relieved, the energy is returned to the axle (accelerating the vehicle). Thus, the concept may be charged from, discharged to, or produce no net effect on a axle that (primarily) rotates in a single direction.

The initial RBLA concept is designed to be installed onto the non-driven shaft of a two-wheel drive vehicle. This will lessen the necessary controls of the system. Sensors must be used to monitor the level of spring charge. While charging or discharging, the spring

deformation will be continually changing, thus the torque affecting the speed of the vehicle will also change. Hence, the RBLA is not designed to be the sole means to propel or stop the vehicle. For example, during launch assist the spring is releasing torque to the non-drive wheels. If the driver desires a higher acceleration, pressing the gas pedal harder will apply torque from the engine to the drive wheels. With differing amounts of torque applied to the wheels, the drive wheels will dictate the speed the car moves, while the RBLA will lessen the torque required. Regenerative braking is a similar scenario, where the brakes aid the spring. The peak acceleration of the RB and LA cycles are limited to standards of comfort, thus it is assumed that the RBLA will aid required accelerations, not define them. Each mode will have the least effect on vehicle speed when the spring is closest to the discharged state, and the greatest effect when the spring is closest to fully charged.

3. DESIGN EQUATIONS

In this section, the equations used to determine appropriate design parameters are formulated.

Vehicle Response to the RBLA

A free body diagram of an automobile of mass m_c being propelled by the RBLA is shown in Fig. 2. The principal vehicle forces include drag F_D, the weight $W = m_c g$, the normal forces on the tires N, and the thrust F_T from the launch assist. The vehicle motion coordinate x_c is also defined in Fig. 2 with velocity $\dot{x}_c$ and acceleration $\ddot{x}_c$. Note that F_T can be either with or against motion $\dot{x}_c$, depending on whether the mechanism is in LA or RB mode.

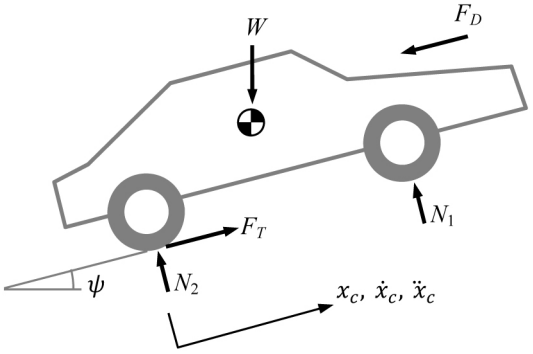

Figure 2. Free body diagram of the vehicle being propelled by the RBLA

Summing the forces along the direction of motion,

$$F_T - F_D - W \sin\psi = m_c \ddot{x}_c. \tag{1}$$

The drag force of the vehicle is dependent on the reference frontal area S, the coefficient of drag C_D, the air density ρ_a and the speed of the air with respect to the vehicle, which is assumed to be the speed of the vehicle $\dot{x}_c$,

$$F_D = \frac{1}{2} C_D \, S \, \rho_a \dot{x}_c{}^2. \tag{2}$$

The torsional energy storage spring has a constant of k_θ and has an angular deflection of θ_s. With a tire radius of r_w, the rotation of the axle is $\theta_w = x_c/r_w$. The angular rotation of Countershaft A, Countershaft B, and the differential carrier are θ_A, θ_B, and θ_D, respectively. The differential carrier exhibits motion that is dictated by $\theta_D = (\theta_A - \theta_B)/2$. The RBLA has velocity ratios between Countershaft A and the axle of $R_A = \theta_A/\theta_w$, between Countershaft B and the axle of $R_B = \theta_B/\theta_w$, and between the differential carrier and the energy storage spring of $R_s = \theta_s/\theta_D$. Note that the ratio for the variable transmission will be changed for brake mode $R_{B_B} > R_A$ and launch mode $R_{B_L} < R_A$. With an initial angular deflection of θ_{s_0}, these ratios form a relationship between the displacement of the car and the spring deflection as

$$x_c = \frac{2 r_w \, (\theta_{s_0} - \theta_s)}{R_s \, (R_A - R_B)}. \tag{3}$$

A spring torque of $k_\theta \theta_s$ produces a torque on the differential carrier of $R_s k_\theta \theta_s$. Transferring that torque through the differential and to the wheel axle gives $R_s \, (R_A - R_B) \, k_\theta \theta_s$. Summing torques on the axle,

$$\frac{1}{2} R_s \, (R_A - R_B) \; k_\theta \, \theta_s - F_T \, r_w = J \, \ddot{\theta}_w, \tag{4}$$

where $\ddot{\theta}_w$ is the acceleration of the axle and J is the effective rotational inertia of the RBLA system along with the wheels. Note that $\ddot{\theta}_w = \ddot{x}_c/r_w$. Substituting into Eq. (4), the thrust force produced by the spring is

$$F_T = \frac{R_s \, (R_A - R_B) \, k_\theta \theta_s}{2 r_w} - \frac{J}{r_w^2} \ddot{x}_c. \tag{5}$$

Substituting Eqs. (5) and (2) into Eq. (1),

$$\frac{R_s \, (R_A - R_B) \, k_\theta \theta_s}{2 r_w} - \frac{J}{r_w^2} \, \ddot{x}_c - \frac{C_D S \rho_a}{2} \dot{x}_c{}^2 - W \sin\psi = m_c \ddot{x}_c. \tag{6}$$

Further substitution of Eq. (3) into Eq. (6) produces the equation of motion for a vehicle launching or braking, when the spring has an initial stretch of θ_{s_0},

$$\left(m_c + \frac{J}{r_w^2}\right)\ddot{x}_c + \frac{C_D\, S\, \rho_a}{2}\dot{x_c}^2 + \frac{R_s^2\,(R_A - R_B)^2\, k_\theta}{4r_w^2}x_c = \frac{R_s\,(R_A - R_B)\, k_\theta \theta_{s_0}}{4r_w} - W\sin\psi. \tag{7}$$

Equation (7) represents a single degree-of-freedom dynamic system and can be used to model both the regenerative brake as well as the launch assist phase of operation. Focusing on a launch, the relatively low speed will allow F_D to be neglected. The solution to Eq. (7), the vehicle response when releasing the spring of initial deformation θ_{s_0}, is

$$x_c = A\,[\cos(\omega\, t + \phi) + 1] \tag{8}$$

where the system natural frequency is

$$\omega = \sqrt{\frac{R_s^2\,(R_A - R_B)^2\, k_\theta}{4(r_w^2\, m_c + J)}}. \tag{9}$$

Control of the variable transmission will prohibit the vehicle response beyond the time where $\theta_s = 0$. If the vehicle is propelled from rest, $\Phi = \pi$. Substituting $x_c = 0$ at $(\omega\, t) = 0$ into Eq. (8),

$$A = \frac{2r_w\theta_{s_0}}{R_s\,(R_A - R_B)} - \frac{2r_w^2 W\sin\psi}{R_s^2\,(R_A - R_B)^2\, k_\theta}. \tag{10}$$

The time derivatives of Eq. (8) are

$$\dot{x}_c = -A\,\omega\sin(\omega\, t - \pi), \tag{11}$$

$$\ddot{x}_c = -A\,\omega^2\cos(\omega\, t - \pi). \tag{12}$$

The vehicle will reach its top speed $\dot{x}_{c_{\max}}$ at time t_s. Observed from Eq. (11) is that $\dot{x}_c$ becomes a maximum when $\omega t_s = \pi/2$. Thus,

$$t_s = \frac{\pi}{2}\sqrt{\frac{4(r_w^2 m_c + J)}{R_s^2\,(R_A - R_B)^2\, k_\theta}}. \tag{13}$$

Also from Eq. (11), the maximum vehicle speed and acceleration obtained by the spring stretch of θ_{s_0} is

$$\dot{x}_{c_{\max}} = -A\omega, \tag{14}$$

$$\ddot{x}_{c_{\max}} = -A\omega^2. \tag{15}$$

Equations (8), (14), and (15) are used to determine the effect of the RBLA on vehicle performance. Both the regenerative phase as well as the launch assist phase can be modeled with these design equations by using the appropriate values of the gear ratios. From the eight variables in the above equations, only three are prescribed vehicle parameters (m_c, J, and r_w), the rest are design variables (R_A, R_B, R_s, k_θ, θ_{s_0}). Note that m_c and J will slightly change with the selection of RBLA components.

EXTENSION SPRING EQUATIONS

For the feasibility study, a torsional steel spring was selected because of its widespread use for storing energy and its ability to safely dissipate energy if failure occurs. For a torsional spring, the spring constant is [17]

$$k_\theta = \frac{d_s^4 E}{64 D_s N_a} \tag{16}$$

where d_s is the spring wire diameter, E is the modulus of elasticity of the spring material, D_s is the mean coil diameter, and N_a is the number of active coils. The length of the spring is approximated as $L_s = N_a d_s$. The maximum bending stress in the wire occurs when the spring is at its maximum angular deformation $\theta_{s_{\max}}$

$$\sigma = \frac{32K_i\,(k_\theta\theta_{s_{\max}})}{\pi\, d_s^3} \tag{17}$$

where K_i is a stress concentration factor,

$$K_i = (4C^2 - C - 1)/4C(C - 1) \tag{18}$$

and $C = D_s/d_s$ is the spring index.

4. SIMULATION

To validate the design equations, a multibody dynamic motion simulation was performed using SolidWorks, a CAD software package. This software has the ability to simulate motions and interaction forces between components. The values used in the model were based on an average consumer sedan, using a 62 cm (24.4 in) wheel diameter and an 1150 kg (2500 lb) vehicle mass. The geometric and mass properties of each component were appropriately specified. The RBLA system dynamic model contains only the moving parts of the device (wheel, shafts, gears, differential carrier, and spring) and is shown in Fig. 3. All other aspects of the design were assumed to be a portion of the vehicle mass and lumped into a single input parameter. The vehicle was constrained to move parallel to the ground, eliminating the need to model the vehicle center of gravity. This neglects any change in vehicle pitch during acceleration.

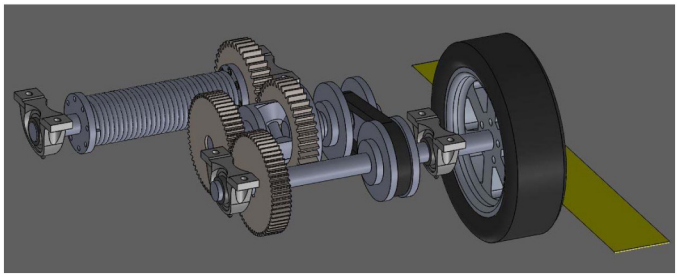

Figure 3. RBLA dynamic simulation model

A launch assist was simulated with the vehicle starting from rest ($\dot{x}_c$=0), expelling spring energy until the spring returns to its undeformed length (θ_s=0). The simulations were conducted on flat pavement (ψ=0) and did not include frictional losses. Additionally, since the maximum launch speed is low, drag forces were not included. For each simulation case, a spring constant k_θ and stretched length θ_{s_0} were specified. The simulation results for R_A = 1, R_{B_L} = 0.4, R_{B_B} = 2, R_s = 1, k_θ = 4.5 N-m/deg, and θ_{s_0} =240° are shown in Fig. 4.

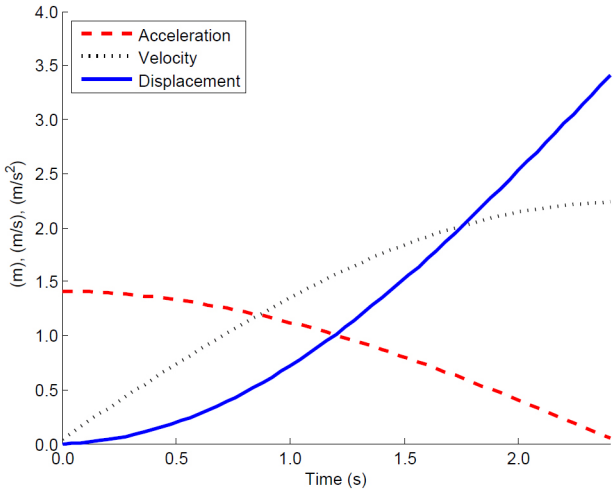

Figure 4. Vehicle response to a spring powered launch assist

Multiple configurations, with different gear ratios and spring parameters, were run in the motion study to validate the design equations. After each configuration was simulated, the vehicle position, velocity, and acceleration were compared to Eqs. (8), (11) and (12), respectively. The simulation results were within 2% of values obtained from the design equations. Differences were attributed to mass properties of the true geometry and the cylindrical representation used in the design equations.

The multibody dynamic model was used to simulate a regenerative brake and launch cycle, such as a vehicle approaching a traffic signal. The simulation begins with the vehicle moving at $\dot{x}_c$ = 6.7 m/s (24 km/hr, 15 mph), when the regenerative brake is engaged. The simulation proceeds through the deceleration of the vehicle to a complete stop. After a 5 second pause, the launch assist is engaged and a subsequent spring-powered acceleration follows. The resulting motion curves are illustrated in Fig. 5 and the results are consistent with Eqs. (8), (11) and (12).

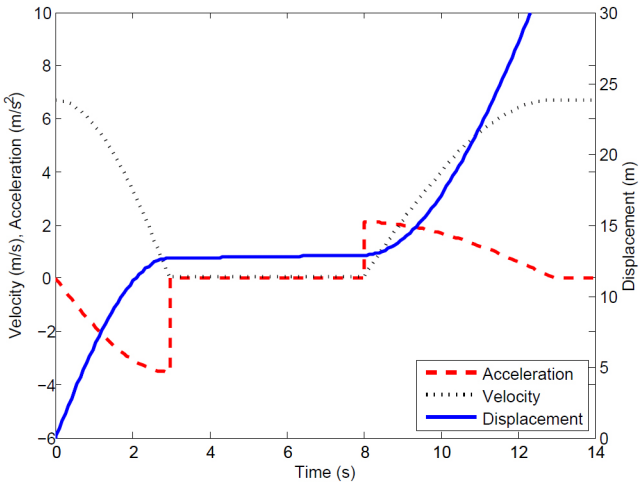

Figure 5. Vehicle response to a regenerative brake and launch cycle

5. OPTIMIZATION

To ideally select the RBLA mechanism design variables (R_A, R_{B_B}, R_{B_L}, R_s, $\theta_{s_{max}}$, N_a, d_s, and D_s), an optimization was preformed using MATLAB's *fmincon* command. This command minimizes a user-defined multivariable objective function subject to constraints. The ultimate goal of the RBLA device is to improve the fuel efficiency of a vehicle. Accordingly, the fuel efficiency was used as the objective. To create a standard, vehicle-independent measure of RBLA benefit, the Environmental Protection Agency (EPA) City Driving Cycle was used.

EPA City Cycle

The EPA City Cycle [15] is a standardized sequence of driving events used to evaluate vehicle fuel consumption. It specifies vehicle speed $\dot{x}_r$ for each second in time over a 22.8 minute course, simulating urban traffic with many accelerations and decelerations. These driving events include 18 stops, an average speed of 32 km/h (20 mph), a top speed of 90 km/h (56 mph), encompassing 12.0 km (7.45 mi). This EPA City Cycle speed profile is shown in Fig. 6 where the vehicle velocity $\dot{x}_{r_i}$ is specified at each of the i = 0,…, 1369 seconds in the profile.

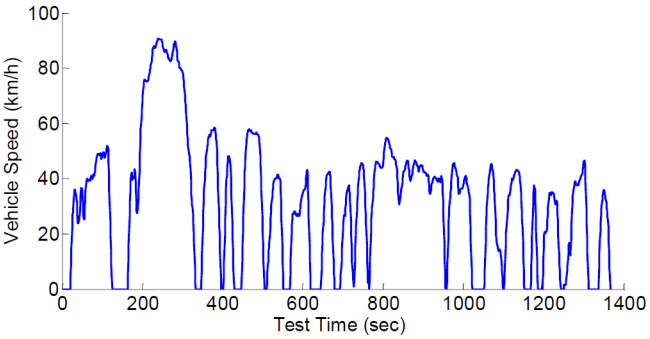

Figure 6. EPA city cycle represented by a vehicle velocity profile

Each positive slope ($\dot{x}_{r_{i+1}} > \dot{x}_{r_i}$) in the driving cycle represents vehicle acceleration, where energy must be supplied to increase the kinetic energy of the vehicle. With a flat terrain and negligible drag forces, the energy required to complete the course is

$$E = \frac{1}{2} m_c \sum_{i=2}^{1369} \left[(\dot{x}_{r_i})^2 - (\dot{x}_{r_{i-1}})^2 \right] \quad \text{iff} \quad \dot{x}_{r_i} > \dot{x}_{r_{i-1}}.$$

(19)

Conversely, each negative slope ($\dot{x}_{r_{i+1}} < \dot{x}_{r_i}$) in the driving cycle represents vehicle deceleration and without regenerative braking, the kinetic energy is dissipated to the environment through the brakes. With the frequent starts and stops, an RBLA installed on a vehicle in this urban setting is expected to have the greatest impact.

RBLA Objective Function

The energy stored and subsequently released by the RBLA on the EPA City Cycle is affected by the RBLA design parameters. Each time the vehicle decelerates, energy will be stored in the spring, until the spring is at its maximum deformation, $\theta_s = \theta_{s_{\max}}$. Likewise, as the vehicle accelerates, energy will be released from the spring until the spring is undeformed, $\theta_s = 0$. Additionally, each acceleration (or deceleration) event may not solely be accomplished by the spring and may require the aid of the engine (or brakes). For each acceleration/deceleration period in the EPA cycle, Eq. (15) provides the vehicle acceleration $\ddot{x}_{c_i}$ that can be obtained by the spring with a deformation of $\theta_{s_{i-1}}$.

At each time increment, the acceleration (or deceleration) prescribed from the EPA Cycle is estimated using the finite difference formula,

$$\ddot{x}_{r_i} = \frac{\dot{x}_{r_i} - \dot{x}_{r_{i-1}}}{t_i - t_{i-1}}.$$

(20)

Similarly, the displacement of the vehicle during the interval from t_{i-1} to t_i as prescribed by the EPA Cycle is estimated using the trapezoidal rule,

$$x_{r_i} - x_{r_{i-1}} = \left[\frac{(\dot{x}_{r_i} + \dot{x}_{r_{i-1}})}{2} \right] (t_i - t_{i-1}).$$

(21)

RB Mode

For any interval when the prescribed vehicle motion involves decceleration ($\ddot{x}_{r_i} < 0$) and the spring is not currently at its maximum stretched length ($\theta_{s_{i-1}} < \theta_{s_{\max}}$), the variable transmission will be shifted to a ratio of $R_{B_B} > R_A$, activating regenerative braking. The spring deflection θ_{s_i} is determined by rewriting Eq. (3) and substituting the vehicle motion

$$\theta_{s_i} = \theta_{s_{i-1}} - \frac{R_s(R_A - R_{B_B})}{2r_w}(x_{r_i} - x_{r_{i-1}}).$$

(22)

The vehicle deceleration attributed to the spring is determined by Eq. (12),

$$\ddot{x}_{c_i} = \frac{R_s(R_A - R_{B_B}) r_w k_\theta \theta_{s_i}}{2(J + m_c r_w^2)}.$$

(23)

If the magnitude of the prescribed deceleration is greater than the deceleration that can be generated by the spring ($|\ddot{x}_{c_i}| < |\ddot{x}_{r_i}|$), the remaining deceleration must be provided by the vehicle brakes. Alternatively, if $|\ddot{x}_{c_i}| > |\ddot{x}_{r_i}|$, the variable transmission ratio will be shifted towards idle mode before the interval is complete in order to achieve $\dot{x}_{r_{i+1}}$. In this case, the spring deflection is determined by rewriting Eq. (12),

$$\theta_{s_i} = \theta_{s_{i-1}} + \frac{2\ddot{x}_{r_i}(J + m_c\, r_w^2)}{R_s\,(R_A - R_{B_B})\, r_w k_\theta}.$$

(24)

If the spring stretch is greater than maximum deformation ($\theta_{s_i} \geq \theta_{s_{\max}}$) in either Eq. (22) or Eq. (24), then the variable transmission is shifted to idle mode, and θ_{s_i} is set to $\theta_{s_{\max}}$.

LA Mode

For any interval when the prescribed vehicle motion involves acceleration ($\ddot{x}_{r_i} > 0$) and the spring is not currently at its minimum deformation ($\theta_{s_{i-1}} > 0$), the variable transmission will be shifted to a ratio of $R_{B_L} < R_A$, initiating the launch assist. The spring deformation is determined in a similar manner as Eq. (22),

$$\theta_{s_i} = \theta_{s_{i-1}} - \frac{R_s(R_A - R_{B_L})}{2r_w}(x_{r_i} - x_{r_{i-1}}),$$

(25)

providing an acceleration produced from the spring as determined from Eq. (12),

$$\ddot{x}_{c_i} = \frac{R_s(R_A - R_{B_L}) r_w k_\theta \theta_{s_i}}{2(J + m_c r_w^2)}.$$

(26)

As before, if the prescribed vehicle acceleration is greater than the spring can provide ($\ddot{x}_{c_i} < \ddot{x}_{r_i}$), the additional acceleration must be provided by the engine. Also, if $\ddot{x}_{c_i} > \ddot{x}_{r_i}$, the variable transmission ratio will be shifted towards idle before the interval is complete. In this case, the spring deflection is determined by rewriting Eq. (12),

$$\theta_{s_i} = \theta_{s_{i-1}} - \frac{2\ddot{x}_{r_i}(J + m_c\, r_w^2)}{R_s\,(R_A - R_{B_L})\, r_w k_\theta}.$$

(27)

If the spring stretch is below the minimum deformation ($\theta_{s_i} \leq 0$) in either Eq. (25) or Eq. (27), then θ_{s_i} will be set to 0.

Once the spring deformation θ_{s_i} during the LA mode is determined from Eq. (25) or Eq. (25), the vehicle velocity attributed to the spring is

$$\dot{x}_{c_i} = \left[\frac{2r_w}{R_s(R_A - R_{B_L})}\right]\left(\frac{\theta_{s_{i-1}} - \theta_{s_i}}{t_i - t_{i-1}}\right). \tag{28}$$

Idle Mode

If the variable transmission is shifted such that $R_B = R_A$, the spring deflection remains unchanged. That is, $\theta_{s_i} = \theta_{s_{i-1}}$ and $\dot{x}_{c_i} = \dot{x}_{c_{i-1}}$.

After the vehicle velocity due to the spring is determined from Eq. (28) at every point in the EPA City Cycle, the total spring energy regenerated from the RBLA to create vehicle acceleration is

$$E_L = \frac{1}{2} m_c \sum_{i=2}^{1368} \left[(\dot{x}_{c_i})^2 - (\dot{x}_{r_{i-1}})^2\right] \quad \text{iff} \quad \dot{x}_{r_i} > \dot{x}_{r_{i-1}}. \tag{29}$$

An example of this exchange of kinetic to spring energy within spring capacity limits is shown in Fig. 7.

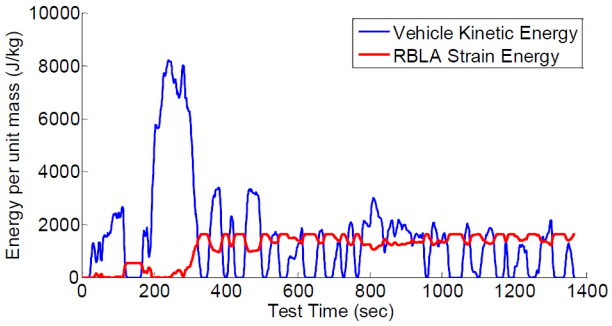

Figure 7. RBLA activity during the EPA city cycle

Energy released from the RBLA corresponds to an amount of gasoline saved, since the engine does not need to produce that energy. The fuel efficiency of a vehicle operating with the RBLA is

$$\eta = \eta_0 \left(1 + \frac{E_L}{E}\right), \tag{30}$$

where η_0 is the fuel efficiency of the vehicle operating without an RBLA.

While increasing the fuel efficiency, the RBLA has a penalty of increasing the mass of the vehicle, which can be modeled as extra payload. Reynolds and Kandlikar [16] quantified a correlation between weight and fuel efficiency for conventional vehicle of approximately 0.7 L/100 km for each additional 100 kg of vehicle mass (0.0018-.0040 mpg/lb). This fuel efficiency penalty ϵ is multiplied by the mass of the RBLA, m_d, which is estimated assuming all gears, shafts, and springs are made of steel and approximated as (potentially hollow) cylinders. Adding the weight penalty to Eq. (30), the estimate for fuel efficiency with an installed RBLA is

$$\eta_{obj} = -\left[\eta_0 \left(1 + \frac{E_L}{E}\right) - \epsilon\, m_d\right]. \tag{31}$$

Equation (31) represents the objective of the optimization and is minimized to determine the ideally sized components for the elastically-based RBLA.

Constraints

The optimization includes multiple constraining functions. The spring dimensions provide the stiffness from Eq. (16), which is used calculating the objective function in Eqs. (23), (24), (26), and (27). An inequality constraint ensures proper performance of the differential, $R_{B_L} < R_A < R_{B_B}$. Another inequality constraint is implemented for reliability. The spring will encounter cyclical stress loading as given in Eq. (17). The spring deformation will be restricted such that the stress is within an acceptable endurance limit for a spring steel (such as ASTM A228), $\sigma \leq 1030$ MPa (150 ksi). Additionally, the spring index C is constrained to $4 \leq C \leq 12$ to facilitate manufacturing.

Throughout the optimization, the size of each rotating component in the RBLA is sized and selected, influencing the mass and effective rotational inertia J of the vehicle drivetrain. Being steel, the spring has a density ρ= 8050 kg/m^3 (0.28 lb/in^3) and a mass of $\pi\rho N_a D_s d_s^2$. All gears and sheaves are considered to have a width of w_g = 25 mm (1.0 in). The fixed ratio input and output gears have diameters of d_{A_1}, and $d_{A_2} = d_{A_1}/R_A$. Likewise, the variable ratio input and output sheaves have diameters of d_{B_1}, and $d_{B_2} = d_{B_1}R_B$. The gear mounted to the differential carrier has a diameter of d_{s_1} and the gear mounted to the torsional spring has a diameter of $d_{s_2} = d_{s_1}/R_s$. Additionally, the differential carrier has an inertia of J_D and wheels of J_w. Combining each component, the effective rotational inertia is

$$J = J_w + \frac{2J_D}{(R_A - R_B)^2} + \frac{\pi}{32}\rho w_g \left[d_{A_1}^4 + d_{B_1}^4 + \frac{d_{A_2}^4}{R_A^2} + \frac{d_{B_2}^4}{R_B^2} + \frac{2d_{s_2}^4}{R_s^2(R_A - R_B)^2}\right]. \tag{32}$$

In addition to the constraints identified, bounds are placed on each design variable as shown in Table 1. Each variable was assigned upper and lower bounds constraining it due to practicality, safety, or manufacturability. For example, the outer diameter of the spring is limited to packaging beneath a vehicle. The completed optimization function produces all design variables as well as the size of all the primary RBLA components.

Optimization Results

The optimal design parameters for an elastically-based RBLA used on an 1150 kg (2500 lb) sedan over the EPA City Driving Cycle are given in Table 1. With modeling assumptions of no vehicle drag, traveling on a flat terrain, and perfect mechanism efficiency, the conventional sedan exhibited an 5.1% increase in the fuel efficiency, from 27.4 city mpg (8.7 L/100 km) to 28.8 mpg (8.0 L/100 km). The optimal spring has an outside diameter of 219 mm (8.6 in), is 933 mm (36.7 in) long and has a mass of 7.1 kg (15.5 lb).

Using the average annual driving miles in the US (418 km, 260 mi) [19] and average fuel price over the past three years (US $3.36) [20], the efficiency gain from the RBLA translates to an annual cost savings of US $81.25. An approximate cost of a high-volume, production version of the RBLA as was estimated as US $325.

The potential of using carbon nanotube (CNT) springs as the energy storage medium within the RBLA device was explored. The CNT springs constructed by Hill et al. are arranged into a hollow tubular structure subjected to torsion [14]. Material properties associated with CNTs include E = 1100 GPa (160.0 Mpsi), μ = 1.4 g/cm^3 (0.05 lb/in^3) and σ_{max} = 32 GPa (4.6 Mpsi). Repeating the optimation resulted in an 18% increase in fuel efficiency for the conventional sedan, equipped with a CNT RBLA device. The optimal spring had a length of 1.49 m (58.66 in), an outer diameter of 0.019 m (0.75 in), an inner diameter of 0.012 m (0.47 in), and a mass of 0.345 kg (0.76 lb).

6. BENCHTOP PROTOTYPE

To confirm the operation of the device, a benchtop prototype was designed as shown in Fig. 8. The axle is fitted with a handle that represents a non-drive wheel. A pair of identical gears are used at Countershaft A, forming a fixed ratio of R_A = 1.0. A bicycle derailleur was used as the variable transmission at Countershaft B. A 16 tooth single sprocket was mounted to the axle. A cassette consisting of 14, 16 and 18 tooth sprockets were mounted to the countershaft. This arrangement provides discrete velocity ratios of R_{B_B}=0.875 (for RB mode), R_B=1.0 (for idle mode), and R_{B_L}=1.125 (for LA mode). Based on availability, a front differential housing from a four wheel drive pickup was used. This differential housing was an ideal choice as it already had the necessary gear connections, bearings, and closely aligned machined structure. To further facilatate prototype fabrication, the torsional spring was replaced with an an extension spring, having stiffness of k_1 = 0.36 N/mm. The end of the spring was attached to a 900 mm (35.43 in) strap that wound around a spool, of radius r_d = 184 mm (7.24 in), which was fastened to the differential housing. A frame was comprised of extruded aluminum.

Testing

The prototype was constructed and is shown in Fig. 9. Testing was performed to evaluate the operation of the prototype. In the initial test, the derailleur was positioned in the idle mode (R_B = 1.0). The axle was rotated and the spring remained in a neutral state. Torque required to rotate the axle in this idle mode was measured as 0.73 N-m (0.54 ft-lb). This measurement characterizes the baseline drag within the mechanism, which is expected to be significantly reduced in a production quality system.

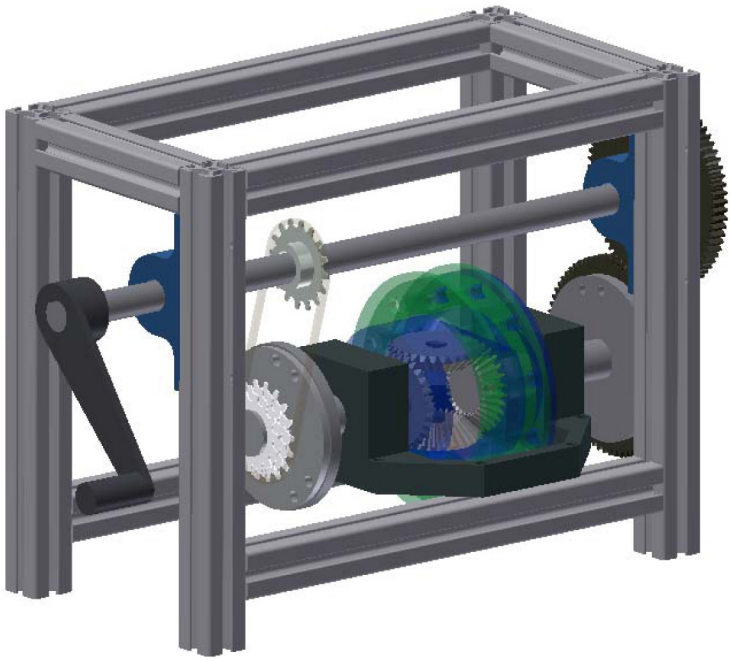

Figure 8. Design model of the RBLA benchtop prototype

In a second series of tests, the derailleur was moved to the brake mode (R_{B_B} = 0.875). The axle was rotated and the spring stretched as expected. Torque required to rotate the axle was measured at different angles. This evaluation was repeated with different spring stiffnesses of k_2 = 0.72 N/mm (4.11 lb/in) and k_3 = 1.44 N/mm (8.22 lb/in) and shown in Fig. 10. Note that the zero-deflection value represents the baseline drag torque of 0.73 N-m. For each spring, a linear relationship between torque and deflection was observed, as provided in Eq. (5). Thus, the braking effect is a linear function of the stiffness and linearly increases as the spring is deformed.

As the derailleur was moved to the launch mode (R_{B_L} = 1.125), the axle was rotated and the spring was returned to its unstretched length. A similar torque measurement was completed to assess the energy is released from the spring.

Table 1. RBLA design optimization parameters

	R_A	R_{B_L}	R_{B_B}	R_s	$\theta_{s_{max}}$	N_a	d_s	D_s
Units	-	-	-	-	rad	-	mm	mm
Lower Bound	0.3	0.4	0.2	0.3	15	20	2	8
Upper Bound	5.0	3.0	7.0	4.0	100	200	20	202
Sedan	2.23	2.04	3.35	0.34	18.8	53.0	17.4	202

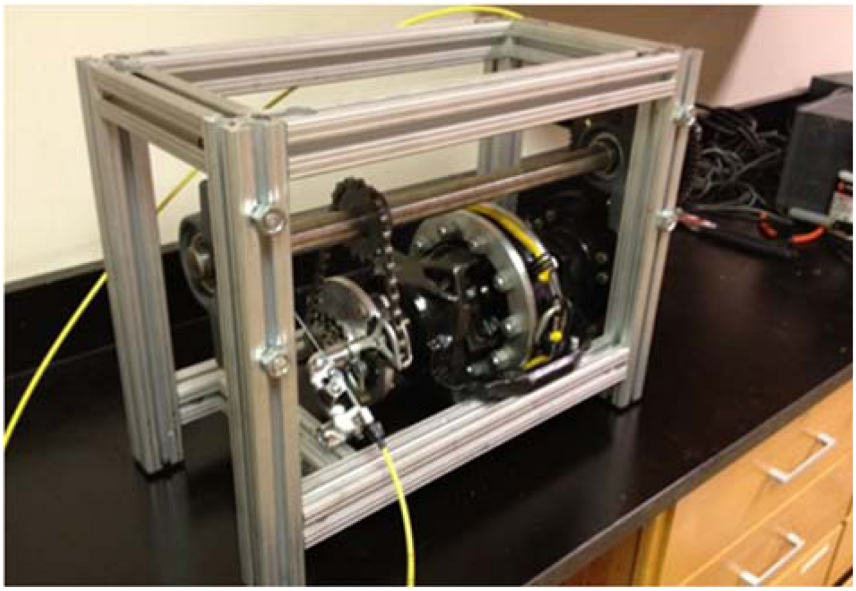

Figure 9. Physical RBLA benchtop prototype

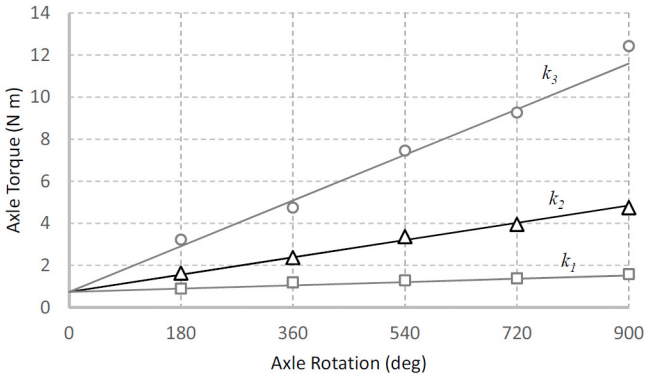

Figure 10. Braking torque while in RB mode

CONCLUSION

This paper presented the conceptual design and development of a novel RBLA with an open differential and elastically-based energy storage. Governing design equations were formulated and verified with commercial dynamic modeling software. To provide the greatest effect on a vehicle, the design equations were posed as an optimization problem. With modeling assumptions that include neglecting vehicle drag and mechanism inefficiencies, the optimization results produced a design that is projected to increase the fuel efficiency of a consumer sedan by 5.1%. A benchtop version of the prototype was designed and constructed for feasibility testing purposes.

REFERENCES

1. Baglione, M., Duty, M., and Pannone, G., "Vehicle System Energy Analysis Methodology and Tool for Determining Vehicle Subsystem Energy Supply and Demand," SAE Technical Paper 2007-01-0398, 2007, doi:10.4271/2007-01-0398.
2. Husain, I. (2011) *Electric and Hybrid Vehicles: Design Fundamentals*, 2/e, CRC Press, Taylor & Francis Group, Boca Raton, FL.
3. Cobb, J. (2014) "December 2013 Dashboard", *HybridCars.com*, Baum & Associates.
4. Abedin, M.J., Masjuki, H. H., Kalam, M. A., Sanjid, A., Ashrafur Rahman, S. M., Masum B. M. (2013) "Energy balance of internal combustion engines using alternative fuels", *Renewable and Sustainable Energy Reviews*, 26(10), pp. 2033
5. Ettefaghi, E., Ahmadi, H., Rashidi, A., Mohtasebi, S. (2013) "Investigation of the Anti-Wear Properties of Nano Additives on Sliding Bearings of Internal Combustion Engines" *International Journal of Precision Engineering and Manufacturing*, 14(5), pp. 805-809.
6. Manning, N., Al-Ghrairi, Vermillion, S. (2013) "Designing a Hydraulic Continously Variable-Transmission (CVT) for Retrofitting a Rear-Wheel Drive Automobile", *Journal of Mechanical Design*, 135(12), 121003.
7. Oleksowicza, S., Burnhama, K., Southgateb, A., McCoyc, C., Waited, G., Hardwicke, G., Harringtonf, C., Ross McMurran, R. (2013) "Regenerative braking strategies, vehicle safety and stability control systems: critical use-case proposals", *Vechicle System Dynamics*, 51(5), pp. 684-699
8. Cross, D. and Brockbank, C., "Mechanical Hybrid System Comprising a Flywheel and CVT for Motorsport and Mainstream Automotive Applications," SAE Technical Paper 2009-01-1312, 2009, doi:10.4271/2009-01-1312.
9. Chiappini, E., "Optimal Use of HLA Systems," SAE Technical Paper 2011-24-0073, 2011, doi:10.4271/2011-24-0073.
10. Hoppie, L.O. (1982) "The Use of Elastomers in Regenerative Braking Systems", *Rubber Chemistry and Technology*, 55(1), pp. 219-232.
11. Nieman, J. E., Myszka, D. H., Murray, A. P., 2014, A Novel, Elastically-Based, Regenerative Brake and Launch Assist Mechanism, *Proc of ASME International Design Engineering Technical Conference*, paper no. DETC 2014-34413.
12. Ashby, M.F. (2011) *Materials Selection in Mechanical Design*, 4/e, Elsevier Ltd., Oxford, U.K.
13. Silva, C., Ross, M., & Farias, T. (2009) "Analysis and simulation of low-cost strategies to reduce fuel consumption and emissions in conventional gasoline light-duty vehicles". *Energy Conversion and Management*, 50(2), 215-222.
14. Hill, F. A., Havel, T., Livermore, C. (2009) "Modeling Mechanical Energy Storage In Springs Based On Carbon Nanotubes", *Nanotechnology*, 20(25), 255704.
15. Environmental Protection Agency (2008) "Urban Dynamometer Drive Schedules", Code of Federal Regulations, Title 40, Reg. 86.
16. Reynolds, C., & Kandlikar, M. (2007) How hybrid-electric vehicles are different from conventional vehicles: the effect of weight and power on fuel consumption. *Environmental Research Letters*, 2(1), 014003.
17. Budynas, R., Nisbett, J. (2010) *Shigley's Mechanical Engineering Design*, 9/e, McGraw-Hill Publishing Company, New York.
18. Gebhard, J. W. (1970) "Acceleration and Comfort in Public Ground Transportation". Johns Hopkins University, Applied Physics Lab., APL/JHU-TPR-002. February. PB 190 402, 49p.

19. Federal Highway Administration (2000) "Average Annual Miles per Driver by Age Group", US Department of Transporation, pub. FHWA-PL-01-1012.
20. Energy Information Administration, (2015) "Motor Average Gasoline Prices", US. Department of Energy.